FACTA UNIVERSITATIS
Series: **Electronics and Energetics** Vol. 31, N° 3, September 2018, pp. 447-460
https://doi.org/10.2298/FUEE1803447S

CHANNEL CAPACITY OF THE MACRODIVERSITY SC SYSTEM IN THE PRESENCE OF KAPPA-MU FADING AND CORRELATED SLOW GAMMA FADING

Marko M. Smilić[1], Branimir S. Jakšić[2], Dejan N. Milić[3], Stefan R. Panić[1], Petar Ć. Spalević[2]

[1]University of Priština, Faculty of Natural Sciences and Mathematics, Kosovska Mitrovica, Serbia
[2]University of Priština, Faculty of Technical Sciences, Kosovska Mitrovica, Serbia
[3]University of Niš, Faculty of Electronic Engineering, Niš, Serbia

Abstract. *In this paper macrodiversity system consisting of two microdiversity SC (Selection Combiner) receivers and one macrodiversity SC receiver are analyzed. Independent κ-μ fading and correlated slow Gamma fading are present at the inputs to the microdiversity SC receivers. For this system model, analytical expression for the probability density of the signal at the output of the macrodiversity receiver SC, and the output capacity of the macrodiversity SC receiver are calculated. The obtained results are graphically presented to show the impact of Rician κ factor, the shading severity of the channel c, the number of clusters μ and correlation coefficient ρ on the probability density of the signal at the output of the macrodiversity system and channel capacity at the output of the macrodiversity system. Based on the obtained results it is possible to analyze the real behavior of the macrodiversity system in the presence of κ-μ fading.*

Key words: *Joint probability density, channel capacity, macrodiversity SC receiver, correlation coefficient, Rician κ factor.*

1. INTRODUCTION

Radio signals generally propagate according to three mechanisms; reflection, diffraction, and scattering. As a result of the above three mechanisms, radio propagation can be roughly characterized by three nearly independent phenomenon; path loss variation with distance, slow log-normal shadowing, and fast multipath fading. Each of these phenomenon is caused by a different underlying physical principle and each must be accounted for when designing and evaluating the performance of a cellular system [1].

Received October 23, 2017; received in revised form February 16, 2018
Corresponding author: Marko M. Smilić
Faculty of Natural Sciences and Mathematics, University of Pristina, Lole Ribara br. 29, 38220 Kosovska Mitrovica, Serbia
(E-mail: marko.smilic@pr.ac.rs)

Fast fading is caused by spreading of signal in multiple directions. The interaction of the waves with objects that are between the transmitter and receiver (reflection, diffraction and dispersion) causes that at the input of the receiver will arrives a large number of copies of the sent signal. The environment through which the wave spreads can be linear and non-linear. When the reflected waves are correlated with factor ρ, the environment is non-linear [1], [2].

Slow fading occurs due to the shadow effect. Various objects between the transmitter and the receiver can form the shadow effect [3]. In most cases, the slow fading is correlated. The signal envelope is variable due to the fast fading, and the power of signal envelope is variable due to the slow fading [4], [5].

The statistical behavior of signals in such systems can be described by different distributions: by Rayleigh, Rician, Nakagami-*m*, Weibull or κ-μ [2], [6], [7]. κ-μ distribution can be used to describe the variation of the signal envelope in linear environments where it is a dominant component. There are several clusters in the propagation environment and the strength of components in phase and quadrature are equal. κ-μ distribution has two parameters. The parameter κ is Rician factor and it is equal to the quotient of the power of dominant component and the power of linear component [8]. Parameter μ is related to the number of clusters in propagation environment. κ-μ distribution is basic distribution, while other distributions can be obtained from it as special cases [9], [10].

A variety of diversity techniques are used to reduce the impact of fast fading and slow fading on system performances. Diversity techniques of more replicas of the same information signal are combined. The most commonly used diversity techniques are MRC (*maximum ratio combining*), EGC (*equal gain combining*) and SC (*selection combining*) [1], [9]. SC diversity receiver is easy for practical realization because the processing is done only on one diversity branch. SC receiver uses the branch with the highest signal-to-noise ratio for next processing of signal [11]. If the noise power is the same in all branches of SC receiver, then SC receiver separates the branch with the strongest signal [6]. Performances of SC receiver are worse than performances of MRC and EGC receivers. At the SC receiver, it is relatively easy to determine probability density and cumulative probability of the signal at the output from the receiver.

The most commonly used are spatial diversity techniques. Spatial diversity techniques are realized with multiple antennas placed on a receiver. By using spatial diversity technique it increases the reliability of the system and the channel capacity without the increase of transmitter power and the expansion of the frequency range. There are more combining spatial diversity techniques that can be used to reduce the influence of fading and co-channel interference on the performance of the system. With regard to analytical methods, for the channel capacity we used the well-known Meijer G-function [12]. It is also shown how with the change of some parameters we influence on the change of the channel capacity.

There are two types of channel capacity: the Shannon capacity and the capacity with outage. Shannon capacity is the maximum data rate that can be sent over the radio channel with asymptotically small error probability, so is also called the ergodic capacity. Capacity with outage is the maximum data rate that can be transmitted over a channel with some outage probability that is the percentage of data that can not be received correctly due to the deep fading [13], [14], [15], [16], [17].

In many papers [18], [19], [20], [21], statistical characteristics of the signal for macrodiversity systems are presented. For the considered system results have not been

presented yet. Based on the results obtained in this paper, it is possible to optimize the parameters of the wireless system and the emission power of the signal. Using the results obtained, it is possible to predict the behavior of various system implementations for various mobile transmission scenarios and in various propagation environments, which enables mobile system designers to make rational system solutions for the desired system performance.

2. SYSTEM MODEL

In this paper we discuss the macrodiversity system with macrodiversity SC (selection combining) receiver and two microdiversity SC receivers. Independent κ-μ fading and slow Gamma fading are at the inputs of the microdiversity SC receivers. The slow fading is correlated. The correlation coefficient decreases with increase of the distance between the antennas.

Microdiversity SC receiver reduces the impact of fast fading on system performance, while macrodiversity SC receiver reduces the impact of slow fading on system performance. Macro system that are discussed here can be used in a single cell of a cellular mobile radio system. Microdiversity receivers are installed on the base stations serving to mobile users in a single cell. Macrodiversity system uses signals from multiple base stations positioned in a single cell or two or more cells.

The system which is discussed is shown in Figure 1.

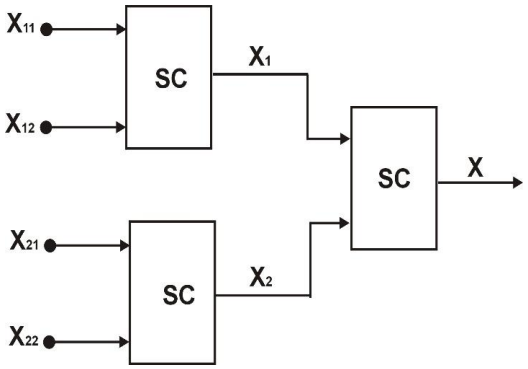

Fig. 1 Macrodiversity system with one macrodiversity SC receiver and two microdiversity SC receivers.

The signals at the input to the first SC microdiversity receiver are marked with x_{11} and x_{12}, and with x_1 at the output. The signals at the input to the other SC microdiversity receiver are marked with x_{21} and x_{22}, and with x_2 at the output. Signal at the output of the macrodiversity system is marked with x. Power of signals at the input to the microdiversity receivers are marked with Ω_1 and Ω_2. The signal at the output of the macrodiversity SC receiver x is equal to the signal at the output of that microdiversity SC receiver whose power is greater than the power of signal at the input of other microdiversity SC receiver [2].

3. THE PROBABILITY DENSITY OF THE SIGNAL

The probability density of κ-μ signal x_1 and first microdiversity SC receiver is given by [22]:

$$p_{x_{1i}}(x_1)=\frac{2\mu(k+1)^{\frac{\mu+1}{2}}}{k^{\frac{\mu-1}{2}}e^{\mu k}\Omega_1^{\mu+1}}x_1^{\mu}e^{-\frac{\mu(k+1)x_1^2}{\Omega_1}}I_{\mu-1}\left(2\mu\sqrt{\frac{k(k+1)}{\Omega_1}}x_1\right),\ i=1,2; \tag{1}$$

The probability density of κ-μ signal x_2 and second microdiversity SC receiver is given by [22]:

$$p_{x_{2i}}(x_2)=\frac{2\mu(k+1)^{\frac{\mu+1}{2}}}{k^{\frac{\mu-1}{2}}e^{\mu k}\Omega_2^{\mu+1}}x_2^{\mu}e^{-\frac{\mu(k+1)x_2^2}{\Omega_2}}I_{\mu-1}\left(2\mu\sqrt{\frac{k(k+1)}{\Omega_2}}x_2\right),\ i=1,2; \tag{2}$$

The parameter μ represents the number of clusters through which the signal is extended, κ Rician factor, Ω_1 and Ω_2 are average power of signals at the output of the first and second microdiversity system respectively, $I_n(\cdot)$ modified Bessel function of the first kind and n type [23]. After using the series for Bessel functions, the term of probability density x_{1i} becomes

$$p_{x_{1i}}(x_1)=\frac{2\mu(k+1)^{\frac{\mu+1}{2}}}{k^{\frac{\mu-1}{2}}e^{\mu k}\Omega_1^{\mu+1}}x_1^{\mu}e^{-\frac{\mu(k+1)x_1^2}{\Omega_1}}\sum_{i_1=0}^{\infty}\left(\mu\sqrt{\frac{k(k+1)}{\Omega_1}}\right)^{2i_1+\mu-1}\frac{1}{i_1!\Gamma(i_1+\mu)}x_1^{2i_1+\mu-1} \tag{3}$$

where $\Gamma(\cdot)$ denotes the Gamma function, and x_{1i} represent signals envelopes at the input of first microdiversity SC receiver and x_1 represents signal envelope at the output of first SC receiver [23].

In a similar way we get the probability density of the signal at the input to another microdiversity SC receiver:

$$p_{x_{2i}}(x_2)=\frac{2\mu(k+1)^{\frac{\mu+1}{2}}}{k^{\frac{\mu-1}{2}}e^{\mu k}\Omega_2^{\mu+1}}x_2^{\mu}e^{-\frac{\mu(k+1)x_2^2}{\Omega_2}}\sum_{i_1=0}^{\infty}\left(\mu\sqrt{\frac{k(k+1)}{\Omega_2}}\right)^{2i_1+\mu-1}\frac{1}{i_1!\Gamma(i_1+\mu)}x_2^{2i_1+\mu-1} \tag{4}$$

The cumulative probability of x_{1i}, i=1,2 is

$$F_{x_{1i}}(x_1)=\int_0^{x_1}dt\,p_{x_1}(t)=\frac{2\mu(k+1)^{\frac{\mu+1}{2}}}{k^{\frac{\mu-1}{2}}e^{\mu k}\Omega_1^{\mu+1}}\sum_{i_2=0}^{\infty}\left(\mu\sqrt{\frac{k(k+1)}{\Omega_1}}\right)^{2i_2+\mu-1}\times \\ \frac{1}{i_2!\Gamma(i_2+\mu)}\int_0^{x_1}dt\cdot t^{2i_2+2\mu-1}e^{-\frac{\mu(k+1)t^2}{\Omega_1}} \tag{5}$$

After solving the integral by the use of [23], we have the expression for the cumulative probability of the signal at the input to the first microdiversity SC receiver:

$$F_{x_{1i}}(x_1)=\frac{\mu(k+1)^{\frac{\mu+1}{2}}}{k^{\frac{\mu-1}{2}}e^{\mu k}\Omega_1^{\mu+1}}\sum_{i_2=0}^{\infty}\left(\mu\sqrt{\frac{k(k+1)}{\Omega_1}}\right)^{2i_2+\mu-1}\frac{1}{i_2!\Gamma(i_2+\mu)}\times \left(\frac{\Omega_1}{\mu(k+1)}\right)^{i_2+\mu}\gamma\left(i_2+\mu,\frac{\mu(k+1)}{\Omega_1}x_1^2\right) \tag{6}$$

where $\gamma(\cdot)$ represents the lower incomplete Gamma function [23]. By applying the procedure for obtaining the cumulative probability of the signal at the input to the first microdiversity SC receiver, the cumulative probability x_{2i} of the signal at the input to the second microdiversity SC receiver can also be obtained. The probability density of the signal at the output of the first microdiversity SC receiver is

$$p_{x_1}(x_1)=p_{x_{11}}(x_1)F_{x_{12}}(x_1)+p_{x_{12}}(x_1)F_{x_{11}}(x_1)=2p_{x_{11}}(x_1)F_{x_{12}}(x_1) \tag{7}$$

where p_{x1i} is given by (3), while F_{x1i} is given by (6). After the replacement of (3) and (6) into (7) we have

$$p_{x_1}(x_1)=4\left(\frac{\mu(k+1)^{\frac{\mu+1}{2}}}{k^{\frac{\mu-1}{2}}e^{\mu k}\Omega_1^{\mu+1}}\right)^2 e^{-\frac{\mu(k+1)x_1^2}{\Omega_1}}\sum_{i_1=0}^{\infty}\left(\mu\sqrt{\frac{k(k+1)}{\Omega_1}}\right)^{2i_1+\mu-1}\frac{1}{i_1!\Gamma(i_1+\mu)}x_1^{2i_1+2\mu-1} \times\sum_{i_2=0}^{\infty}\left(\mu\sqrt{\frac{k(k+1)}{\Omega_1}}\right)^{2i_2+\mu-1}\frac{1}{i_2!\Gamma(i_2+\mu)}\left(\frac{\Omega_1}{\mu(k+1)}\right)^{i_2+\mu}\gamma\left(i_2+\mu,\frac{\mu(k+1)}{\Omega_1}x_1^2\right) \tag{8}$$

The probability density of the signal at the output of the second microdiversity SC receiver is

$$p_{x_2}(x_2)=4\left(\frac{\mu(k+1)^{\frac{\mu+1}{2}}}{k^{\frac{\mu-1}{2}}e^{\mu k}\Omega_2^{\mu+1}}\right)^2 e^{-\frac{\mu(k+1)x_2^2}{\Omega_2}}\sum_{i_1=0}^{\infty}\left(\mu\sqrt{\frac{k(k+1)}{\Omega_2}}\right)^{2i_1+\mu-1}\frac{1}{i_1!\Gamma(i_1+\mu)}y_2^{2i_1+2\mu-1} \times\sum_{i_2=0}^{\infty}\left(\mu\sqrt{\frac{k(k+1)}{\Omega_2}}\right)^{2i_2+\mu-1}\frac{1}{i_2!\Gamma(i_2+\mu)}\left(\frac{\Omega_2}{\mu(k+1)}\right)^{i_2+\mu}\gamma\left(i_2+\mu,\frac{\mu(k+1)}{\Omega_2}x_2^2\right) \tag{9}$$

Probability density of the signal at the output of macrodiversity SC receiver is equal to the probability density of the signal at the output of that microdiversity SC receiver whose power at the input is greater than the power of the signal at the input to the two other microdiversity SC receivers [23]. Based on this, the probability density of the signal at the output of the microdiversity SC receiver is equal to

$$p_x(x)=\int_0^{\infty}d\Omega_1\int_0^{\Omega_1}d\Omega_2\,p_{x_1}(x/\Omega_1)p_{\Omega_1\Omega_2}(\Omega_1\Omega_2)+ \int_0^{\infty}d\Omega_1\int_0^{\Omega_1}d\Omega_2\,p_{x_2}(x/\Omega_1)p_{\Omega_1\Omega_2}(\Omega_1\Omega_2)=I_1+I_2 \tag{10}$$

where $p_x(x/\Omega_1)$, $p_x(x/\Omega_2)$ are given by (8) and (9), respectively. Joint probability density power Ω_1, Ω_2 is given by [6]:

$$p_{\Omega_1\Omega_2}(\Omega_1\Omega_2)=\frac{1}{\Gamma(c)(1-\rho^2)\rho^{c-1}\Omega_0^{c+2}}\sum_{i_3=0}^{\infty}\left(\frac{\sqrt{\rho}}{\Omega_0(1-\rho)}\right)^{2i_3+c-1}\times \\ \frac{1}{i_3!\Gamma(i_3+c)}\Omega_1^{i_3+c-1}\Omega_2^{i_3+c-1}e^{-\frac{\Omega_1+\Omega_2}{\Omega_0(1-\rho)}} \tag{11}$$

where c is shadowing severity.

Integral I_1 is equal to

$$I_1=\int_0^{\infty}d\Omega_1\int_0^{\Omega_1}d\Omega_2\,p_{x_1}(x/\Omega_1)\,p_{\Omega_1\Omega_2}(\Omega_1\Omega_2)=4\left(\frac{\mu(k+1)^{\frac{\mu+1}{2}}}{k^{\frac{\mu-1}{2}}e^{\mu k}}\right)^2\sum_{i_1=0}^{\infty}\left(\mu\sqrt{k(k+1)}\right)^{2i_1+\mu-1} \\ \times x^{2i_1+2\mu-1}\frac{1}{i_1!\Gamma(i_1+\mu)}\times\sum_{i_2=0}^{\infty}\left(\mu\sqrt{k(k+1)}\right)^{2i_2+\mu-1}\frac{1}{i_2!\Gamma(i_2+\mu)}\frac{1}{(\mu(k+1))^{i_2+\mu}} \\ \times\gamma\left(i_2+\mu,\frac{\mu(k+1)}{\Omega_1}x^2\right)\frac{1}{\Gamma(c)(1-\rho^2)\rho^{c-1}\Omega_0^{c+2}}\sum_{i_3=0}^{\infty}\left(\frac{\sqrt{\rho}}{\Omega_0(1-\rho)}\right)^{2i_3+c-1}\frac{1}{i_3!\Gamma(i_3+c)} \\ \times\int_0^{\infty}d\Omega_1\Omega_1^{i_3+c-1-i_1-\frac{\mu}{2}+\frac{1}{2}-i_2-\frac{\mu}{2}+\frac{1}{2}-2\mu-2+i_2+\mu}e^{-\frac{\mu(k+1)x^2}{\Omega_1}\frac{\Omega_1}{\Omega_0(1-\rho)}}\int_0^{\Omega_1}d\Omega_2\Omega_2^{i_3+c-1}e^{-\frac{\Omega_2}{\Omega_0(1-\rho)}} \tag{12}$$

By the use of the method for calculating the integral I_1 (Appendix A, expressions A1, A2 and A3), the integral I_2 is also solved:

$$I_2=\int_0^{\infty}d\Omega_1\int_0^{\Omega_1}d\Omega_2\,p_{x_2}(x/\Omega_1)\,p_{\Omega_1\Omega_2}(\Omega_1\Omega_2) \tag{13}$$

4. CHANNEL CAPACITY OF MACRODIVERSITY

After we got the expression for the joint probability density, we can calculate channel capacity at the output of the macrodiversity system shown in Figure 1. The maximum data rate can be achieved after the channel has experienced all possible fading states during a sufficiently long transmitting time, which can be expressed as follows in the unit of bits per second, where B denotes channel bandwidth expressed in Hz [24], [25]:

$$C=B\int_0^{\infty}log_2(1+x)\,p_x(x)dx \tag{14}$$

Substituting the expression for the joint probability density in the expression for the channel capacity, we get:

$$\frac{C}{B}=\frac{4}{\ln 2}\int_0^\infty dx\ln(1+x)\left(\frac{\mu(k+1)^{\frac{\mu+1}{2}}}{k^{\frac{\mu-1}{2}}e^{\mu k}}\right)^2\sum_{i_1=0}^{\infty}\left(\mu\sqrt{k(k+1)}\right)^{2i_1+\mu-1}x^{2i_1+2\mu-1}\frac{1}{i_1!\Gamma(i_1+\mu)}$$
$$\times\sum_{i_2=0}^{\infty}\left(\mu\sqrt{k(k+1)}\right)^{2i_2+\mu-1}\frac{1}{i_2!\Gamma(i_2+\mu)}\frac{1}{(\mu(k+1))^{i_2+\mu}}\frac{1}{\Gamma(c)(1-\rho^2)\rho^{c-1}\Omega_0^{c+2}}$$
$$\times\sum_{i_3=0}^{\infty}\left(\frac{\sqrt{\rho}}{\Omega_0(1-\rho)}\right)^{2i_3+c-1}\frac{1}{i_3!\Gamma(i_3+c)}\frac{1}{i_3+c}\sum_{j_1=0}^{\infty}\frac{(i_3+c)!}{(i_3+c+j_1)!}\frac{1}{(\Omega_0(1-\rho))^{j_1}}\frac{1}{i_2+\mu} \tag{15}$$
$$\times(\mu(k+1)x^2)^{i_2+\mu}\sum_{j_2=0}^{\infty}\frac{(i_2+\mu)!}{(i_2+\mu+j_2)!}(\mu(k+1)x^2)^{j_2}(2\mu(k+1)x^2\Omega_0(1-\rho))^{\frac{-i_1-i_2+2i_3+j_1-j_2-3\mu+2c-1}{2}}$$
$$\times K_{-i_1-i_2+2i_3+j_1-j_2-3\mu+2c-1}\left(2\sqrt{\frac{4\mu(k+1)x^2}{\Omega_0(1-\rho)}}\right)$$

In order to make the integral solution from expression (15) simpler, firstly, in front of the integrals we can get all the constants, ie, everything that does not solve the integral. Secondly, we can show the logarithmic function through Meijer G-function (Appendix B, expression B1) as well as Bessel function (Appendix B, expressions B2 and B3), with the aim to get more convenient and simpler expression for resolution. The general form of our expression for the channel capacity would be:

$$\frac{C}{B}=R\int_0^\infty dx x^r\ln(1+x)K_v\left(x\right) \tag{16}$$

where *R* represents a constant, or an expression in front of the integral, *r* represents the argument of degree variable by which the expression is solved and *v* represents the argument of Bessel function.

Replacing (B5) into (B4), we get the expression for the solution of channel capacity at the output of the macrodiversity system:

$$\frac{C}{B}=2\frac{2^{z-1}}{2\pi}\left(\frac{\mu(k+1)^{\frac{\mu+1}{2}}}{k^{\frac{\mu-1}{2}}e^{\mu k}}\right)^2\sum_{i_1=0}^{\infty}\left(\mu\sqrt{k(k+1)}\right)^{2i_1+\mu-1}\frac{1}{i_1!\Gamma(i_1+\mu)}\sum_{i_2=0}^{\infty}\left(\mu\sqrt{k(k+1)}\right)^{2i_2+\mu-1}\frac{1}{i_2!\Gamma(i_2+\mu)}$$
$$\times\frac{1}{(\mu(k+1))^{i_2+\mu}}\frac{1}{\Gamma(c)(1-\rho^2)\rho^{c-1}\Omega_0^{c+2}}\sum_{i_3=0}^{\infty}\left(\frac{\sqrt{\rho}}{\Omega_0(1-\rho)}\right)^{2i_3+c-1}\frac{1}{i_3!\Gamma(i_3+c)}\frac{1}{i_3+c} \tag{17}$$
$$\times\sum_{j_1=0}^{\infty}\frac{(i_3+c)!}{(i_3+c+j_1)!}\frac{1}{(\Omega_0(1-\rho))^{j_1}}\frac{1}{i_2+\mu}(\mu(k+1))^{i_2+\mu}\sum_{j_2=0}^{\infty}\frac{(i_2+\mu)!}{(i_2+\mu+j_2)!}(\mu(k+1)x^2)^{j_2}$$
$$\times(2\mu(k+1)\Omega_0(1-\rho))^{\frac{-i_1-i_2+2i_3+j_1-j_2-3\mu+2c-1}{2}}G_{46}^{62}\left[\frac{4\mu(k+1)}{\Omega_0(1-\rho)}\middle|\begin{matrix}\Delta(l,1-\alpha-d_s),\Delta(l,1-\alpha-d_v)\\ b_1,b_m,\Delta(l,1-\alpha-c_1),\Delta(l,1-\alpha-c_t)\end{matrix}\right]$$

In Table 1, the number of terms to be summed in order to achieve accuracy at the desired significant digit is depicted. As we can see from the table, how increases the correlation coefficient increases the number of terms to be summed in order to achieve accuracy at the 4th significant digit. For higher values of parameter *c*, smaller number of terms to achieve accuracy at the 4th significant digit is required [2], [26].

Table 1 Terms need to be summed in the expression for cumulative distribution function to achieve accuracy at the significant digit presented in the brackets.

x=1, k=1, Ω_0=1	c=1 (4th)	c=1.5 (4th)	c=2 (4th)
P=0.2	148	132	118
P=0.4	152	138	121
P=0.6	154	140	125
P=0.8	155	141	126

5. NUMERICAL RESULTS

By using (12) and (13), in Figure 2 we show the change of the probability density of the signal x at the output of the macrodiversity system for different number of clusters μ through which the signal extends. Medium powers of signal are Ω_0 = 1, the correlation coefficient ρ = 0.5, shadowing severity c = 1.5 and Rician factor κ=1. In the figure we can see that the highest value of the probability density for value parameter μ. With the decrease of μ number of clusters, decrease in the probability density of the signal is slower. In the figure we can see that maximum values of the probability density for higher values of parameter μ. With the decrease of μ number of clusters, decrease in the probability density of the signal is slower.

Also, by using (12) and (13), in Figure 3 we show the probability density of the signal x at the output of macrodiversity system for different values of Rician κ factor and μ number of clusters. Medium power of signals are Ω_0= 1, the correlation coefficient ρ = 0.5, and the channel shadowing severity c = 1.5. For higher values of parameter κ and μ are obtained more extreme of the probability density and its faster decrease.

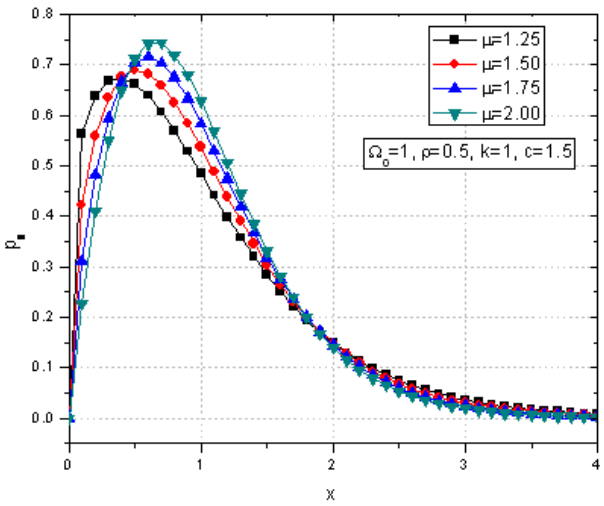

Fig. 2 The probability density of the signal at the output of macrodiversity SC receiver for different values of μ number of clusters.

By using (17), in Figure 4 we show the channel capacity depending on the correlation coefficient at the output of macrodiversity system for various numbers of cluster μ and the channel shadowing severity *c*. Medium powers of signal are $\Omega_0 = 1$, and Rician factor κ=1. We can see in the figure that the channel capacity decreases with the correlation coefficient at the output of macrodiversity system. For lower values of the correlation coefficient, the highest capacity channel is obtained for higher values of μ number of clusters and the channel shadowing severity *c*, but channel capacity faster decreases for the same values than for lower values of μ number of clusters and the channel shadowing severity *c*.

For lower values of the correlation coefficient, the highest capacity channel is obtained for higher values of μ number of clusters and the channel shadowing severity *c*, but channel capacity faster decreases for the same values than for lower values of μ number of clusters and the channel shadowing severity *c*.

Figure 5 gives the graphic view of the channel capacity at the output of the macrodiversity system depending on Rician κ factor for different values of μ number of cluster. Medium powers of the signal are $\Omega_0 = 1$, the channel shadowing severity $c = 1$. Channel capacity at the output of macrodiversity system decreases with the increase of Rician κ factor especially in his lower values, while for higher values the mean number of axial cross sections is constant and approximately equal, regardless of the number of clusters. Channel capacity faster decreases for lower values of the number of clusters.

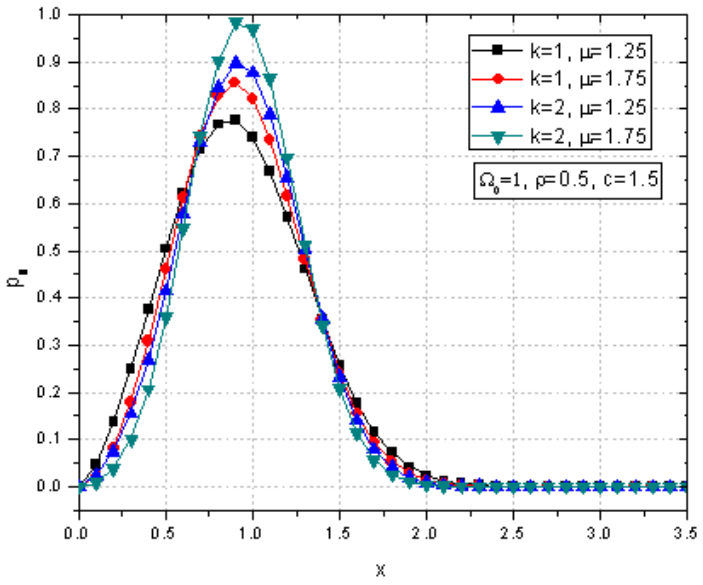

Fig. 3 The probability density of the signal at the output of macrodiversity SC receiver for different values of Rician κ factor and μ number of clusters.

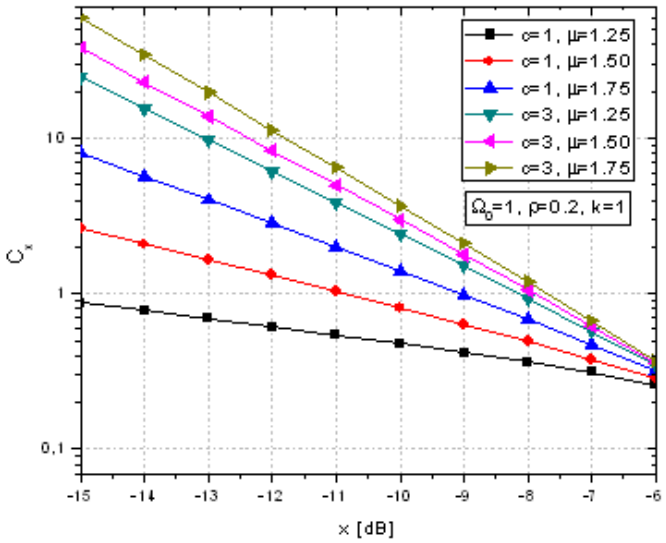

Fig. 4 Channel capacity per unit bandwidth at the output of the macrodiversity SC receiver for different values of the channel shadowing severity *c* and μ number of clusters.

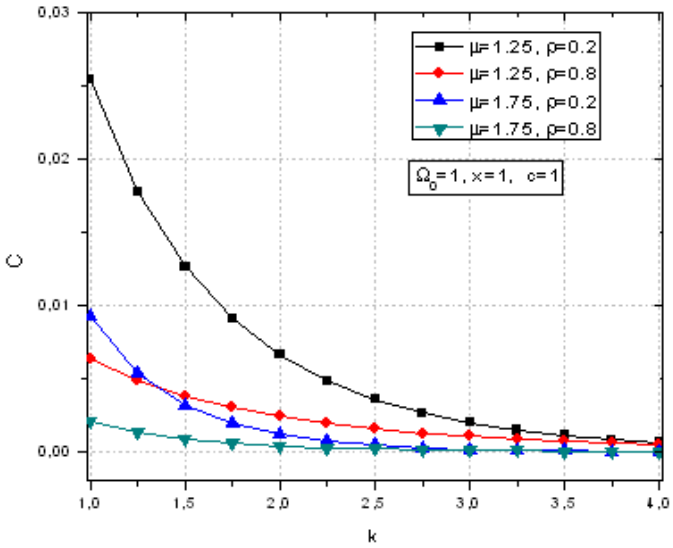

Fig. 5 Channel capacity per unit bandwidth at the output of macrodiversity system depending on the Rician κ factor.

6. CONCLUSION

In this paper we discussed the diversity system with two microdiversity SC receivers and one macrodiversity SC receiver. At the inputs to microdiversity SC receivers there is an independent κ-μ fading and correlated slow Gamma fading. Microdiversity SC receiver reduces the impact of fast fading on system performances, while macrodiversity SC receiver reduces the impact of slow fading on system performances.

For this system, the probability density function and channel capacity at the output from the macrodiversity system are calculated. The probability density of the signal is important statistical characteristic through which we calculate other statistical characteristics of the first and the second order. When the parameter μ decreases, acuity fading influence increases, but when the parameter μ increases, acuity fading influence decreases. When the acuity fading influence increases, system performances deteriorate. Greater acuity fading influence occurs when Rician κ factor is smaller.

For lower values of the correlation coefficient, the highest channel capacity is obtained for higher values of μ number of clusters and the channel shadowing severity *c*. Channel capacity at the output of macrodiversity system decreases with the increase of Rician κ factor especially in his lower values, while for higher values the mean number of axial cross-sections is constant and approximately equal, regardless of the number of clusters. The analysis presented in this paper has a high level of generality and applicability, due to the fact that the modeling of propagation scenarios performed using κ-μ model, which within itself, as a special case involves a large number of known signal propagation model (Nakagami-*m*, Rayleigh, Rician etc…).

APPENDIX A

After using [21] for solving the second integral in (12), I_1 becomes:

$$\begin{aligned} I_1 = 4\left(\frac{\mu(k+1)^{\frac{\mu+1}{2}}}{k^{\frac{\mu-1}{2}}e^{\mu k}}\right)^2 \sum_{i_1=0}^{\infty}\left(\mu\sqrt{k(k+1)}\right)^{2i_1+\mu-1} x^{2i_1+2\mu-1} \frac{1}{i_1!\Gamma(i_1+\mu)} \sum_{i_2=0}^{\infty}\left(\mu\sqrt{k(k+1)}\right)^{2i_2+\mu-1} \\ \times \frac{1}{i_2!\Gamma(i_2+\mu)} \frac{1}{(\mu(k+1))^{i_2+\mu}} \frac{1}{\Gamma(c)(1-\rho^2)\rho^{c-1}\Omega_0^{c+2}} \sum_{i_3=0}^{\infty}\left(\frac{\sqrt{\rho}}{\Omega_0(1-\rho)}\right)^{2i_3+c-1} \\ \times \frac{1}{i_3!\Gamma(i_3+c)} \times (\Omega_0(1-\rho))^{i_3+c} \gamma\left(i_2+\mu, \frac{\mu(k+1)}{\Omega_1}x^2\right) \gamma\left(i_3+c, \frac{\Omega_1}{\Omega_0(1-\rho)}\right) \\ \times \int_0^{\infty} d\Omega_1 \Omega_1^{i_3+c-1-i_1-\frac{\mu}{2}+\frac{1}{2}-i_2-\frac{\mu}{2}+\frac{1}{2}-2\mu-2+i_2+\mu} e^{-\frac{\mu(k+1)x^2}{\Omega_1}-\frac{\Omega_1}{\Omega_0(1-\rho)}} \end{aligned} \tag{A1}$$

After the development of Gamma function

$$\gamma(n,x) = \frac{1}{n}x^n e^{-x}\sum_{i=0}^{\infty}\frac{n!}{(n+i)!}x^i \tag{A2}$$

And by the use of [21] we have

$$I_1 = 4\left(\frac{\mu(k+1)^{\frac{\mu+1}{2}}}{k^{\frac{\mu-1}{2}}e^{\mu k}}\right)^2 \sum_{i_1=0}^{\infty}\left(\mu\sqrt{k(k+1)}\right)^{2i_1+\mu-1} x^{2i_1+2\mu-1}\frac{1}{i_1!\Gamma(i_1+\mu)}\sum_{i_2=0}^{\infty}\left(\mu\sqrt{k(k+1)}\right)^{2i_2+\mu-1}$$
$$\times\frac{1}{i_2!\Gamma(i_2+\mu)}\frac{1}{(\mu(k+1))^{i_2+\mu}}\frac{1}{\Gamma(c)(1-\rho^2)\rho^{c-1}\Omega_0^{c+2}}\sum_{i_3=0}^{\infty}\left(\frac{\sqrt{\rho}}{\Omega_0(1-\rho)}\right)^{2i_3+c-1}$$
$$\times\frac{1}{i_3!\Gamma(i_3+c)}\frac{1}{i_3+c}\sum_{j_1=0}^{\infty}\frac{(i_3+c)!}{(i_3+c+j_1)!}\frac{1}{(\Omega_0(1-\rho))^{j_1}}\frac{1}{i_2+\mu}(\mu(k+1)x^2)^{i_2+\mu} \qquad \text{(A3)}$$
$$\times\sum_{j_2=0}^{\infty}\frac{(i_2+\mu)!}{(i_2+\mu+j_2)!}(\mu(k+1)x^2)^{j_2}(2\mu(k+1)x^2\Omega_0(1-\rho))^{\frac{-i_1-i_2+2i_3+j_1-j_2-3\mu+2c-1}{2}}$$
$$\times K_{-i_1-i_2+2i_3+j_1-j_2-3\mu+2c-1}\left(2\sqrt{\frac{4\mu(k+1)x^2}{\Omega_0(1-\rho)}}\right)$$

where $K_n(x)$ is modified Bessel's function of the second kind, order n and argument x [21]. Infinite-series from above rapidly converge with only few terms needed to achieve accuracy at 5th significant digit.

APPENDIX B

By applying from [27] we have:

$$\ln(1+x) = G_{22}^{12}\left[x\,\middle|\,\begin{matrix}1,1\\1,0\end{matrix}\right] \qquad \text{(B1)}$$

And by applying the formula (8.4.23/1) from [24] we have:

$$K_\nu(x) = \frac{1}{2}G_{02}^{20}\left[\frac{x^2}{4}\,\middle|\,\begin{matrix}-\\ \frac{\nu}{2},-\frac{\nu}{2}\end{matrix}\right] \qquad \text{(B2)}$$

specifically for our case the application of (20) would be:

$$K_{-i_1-i_2+2i_3+j_1-j_2-3\mu+2c-1}\left(2\sqrt{\frac{4\mu(k+1)x^2}{\Omega_0(1-\rho)}}\right) = \frac{1}{2}G_{02}^{20}\left[\frac{4\mu(k+1)x^2}{\Omega_0(1-\rho)}\,\middle|\,\begin{matrix}-,-\\ b_1,b_m\end{matrix}\right]$$
$$b_1 = \frac{-i_1-i_2+2i_3+j_1-j_2-3\mu+2c-1}{2}; \qquad \text{(B3)}$$
$$b_m = \frac{i_1+i_2-2i_3-j_1+j_2+3\mu-2c+1}{2}.$$

After replacing (B1) and (B3) into (15) and after arrangement, we get the expression:

$$\begin{aligned}\frac{C}{B}=4(&\frac{\mu(k+1)^{\frac{\mu+1}{2}}}{k^{\frac{\mu-1}{2}}e^{\mu k}})^2\sum_{i_1=0}^{\infty}\left(\mu\sqrt{k(k+1)}\right)^{2i_1+\mu-1}\frac{1}{i_1!\Gamma(i_1+\mu)}\sum_{i_2=0}^{\infty}\left(\mu\sqrt{k(k+1)}\right)^{2i_2+\mu-1}\\ &\times\frac{1}{i_2!\Gamma(i_2+\mu)}\frac{1}{(\mu(k+1))^{i_2+\mu}}\frac{1}{\Gamma(c)(1-\rho^2)\rho^{c-1}\Omega_0^{c+2}}\sum_{i_3=0}^{\infty}\left(\frac{\sqrt{\rho}}{\Omega_0(1-\rho)}\right)^{2i_3+c-1}\\ &\times\frac{1}{i_3!\Gamma(i_3+c)}\frac{1}{i_3+c}\sum_{j_1=0}^{\infty}\frac{(i_3+c)!}{(i_3+c+j_1)!}\frac{1}{(\Omega_0(1-\rho))^{j_1}}\frac{1}{i_2+\mu}(\mu(k+1))^{i_2+\mu}\\ &\times\sum_{j_2=0}^{\infty}\frac{(i_2+\mu)!}{(i_2+\mu+j_2)!}(\mu(k+1)x^2)^{j2}(2\mu(k+1)\Omega_0(1-\rho))^{\frac{-i_1-i_2+2i_3+j_1-j_2-3\mu+2c-1}{2}}\\ &\times\int_0^{\infty}dx x^{i_1+i_2+2i_3+j_1+j_2+\mu+2c-2}G_{22}^{12}\left[x\,|\,\begin{matrix}1,1\\1,0\end{matrix}\right]\frac{1}{2}G_{02}^{20}\left[\frac{4\mu(k+1)x^2}{\Omega_0(1-\rho)}\,|\,\begin{matrix}-,-\\b_1,b_m\end{matrix}\right]\end{aligned}\tag{B4}$$

Integral of (B4) is solved by applying the formula (2.24.1/1) from [24]. We get that the integral is equal to:

$$\begin{aligned}I&=\int_0^{\infty}dx x^{i_1+i_2+2i_3+j_1+j_2+\mu+2c-2}G_{22}^{12}\left[x\,|\,\begin{matrix}1,1\\1,0\end{matrix}\right]\frac{1}{2}G_{02}^{20}\left[\frac{4\mu(k+1)x^2}{\Omega_0(1-\rho)}\,|\,\begin{matrix}-,-\\b_1,b_m\end{matrix}\right]\\&=\frac{1}{2}\frac{2^{z-1}}{2\pi}G_{46}^{62}\left[\frac{4\mu(k+1)}{\Omega_0(1-\rho)}\,|\,\begin{matrix}\Delta(l,1-\alpha-d_s),\Delta(l,1-\alpha-d_v)\\b_1,b_m,\Delta(l,1-\alpha-c_1),\Delta(l,1-\alpha-c_t)\end{matrix}\right]\\ \Delta(l,1-\alpha-d_s)&=\frac{1-i_1-i_2-2i_3-j_1-j_2-\mu-2c}{2};\Delta(l,1-\alpha-d_s)=\frac{2-i_1-i_2-2i_3-j_1-j_2-\mu-2c}{2};\\ \Delta(l,1-\alpha-d_v)&=\frac{2-i_1-i_2-2i_3-j_1-j_2-\mu-2c}{2};\Delta(l,1-\alpha-d_v)=\frac{3-i_1-i_2-2i_3-j_1-j_2-\mu-2c}{2};\\ b_1&=\frac{-i_1-i_2+2i_3+j_1-j_2-3\mu+2c-1}{2};b_m=\frac{i_1+i_2-2i_3-j_1+j_2+3\mu-2c+1}{2};\\ \Delta(l,1-\alpha-c_1)&=\frac{1-i_1-i_2-2i_3-j_1-j_2-\mu-2c}{2};\Delta(l,1-\alpha-c_1)=\frac{2-i_1-i_2-2i_3-j_1-j_2-\mu-2c}{2};\\ \Delta(l,1-\alpha-c_t)&=\frac{1-i_1-i_2-2i_3-j_1-j_2-\mu-2c}{2};\Delta(l,1-\alpha-c_t)=\frac{2-i_1-i_2-2i_3-j_1-j_2-\mu-2c}{2}.\end{aligned}\tag{B5}$$

REFERENCES

[1] G. L. Stüber, *Principles of mobile communication*, 2nd ed. New York: Kluwer Academic Publishers, 2002.

[2] S. Panic, M. Stefanovic, J. Anastasov, and P. Spalevic, *Fading and Interference Mitigation in Wireless Communications*, 1st ed. Boca Raton, FL, USA: CRC Press, Inc., 2013.

[3] M. K. Simon and M.-S. Alouini, *Digital Communication over Fading Channels*, 2nd ed. New York: John Wiley & Sons, Inc., 2005.

[4] S. R. Panić, D. M. Stefanović, I. M. Petrović, M. Č. Stefanović, J. A. Anastassov, and D. S. Krstić, "Second order statistics of selection macro-diversity system operating over gamma shadowed κ-μ fading channels," *EURASIP J. Wirel. Commun. Netw.*, vol. 2011, no. 151, pp. 1–7, 2011.

[5] M. D. Yacoub, "The κ-μ distribution and the η-μ distribution," *IEEE Antennas Propag. Mag.*, vol. 49, no. 1, pp. 68–81, 2007.

[6] N. Djordjević, B. S. Jakšić, A. Matović, M. Matović, and M. Smilić, "Moments of microdiversity egc receivers and macrodiversity sc receiver output signal over gamma shadowed nakagami-mmultipath fading channel," *J. Electr. Eng.*, vol. 66, no. 6, pp. 348–351, 2015.
[7] A. V. Marković, Z. H. Perić, D. B. Đošić, M. M. Smilić, and B. S. Jakšić, "Level Crossing Rate of Macrodiversity System Over Composite Gamma Shadowed Alpha-Kappa-Mu Multipath Fading Channel," *Facta Universitatis, Ser. Autom. Control Robot.*, vol. 14, no. 2, pp. 99–109, 2015.
[8] D. Krstic, V. Doljak, M. Stefanovic, and B. Jaksic, "Second order statistics of macrodiversity SC receiver output signal over Gamma shadowed K-μ multipath fading channel," in *Proceedings of the 2016 International Conference on Broadband Communications for Next Generation Networks and Multimedia Applications (CoBCom)*, 2016, pp. 1–6.
[9] J. Proakis, *Digital Communications*, 4th ed. New York: McGraw-Hill, 2001.
[10] P. M. Shankar, "Analysis of microdiversity and dual channel macrodiversity in shadowed fading channels using a compound fading model," *AEU - Int. J. Electron. Commun.*, vol. 62, no. 6, pp. 445–449, Jun. 2008.
[11] P. C. Spalevic, B. S. Jaksic, B. P. Prlincevic, I. Dinic, and M. M. Smilic, "Signal Moments at the Output from the Macrodiversity System with Three MRC Micro Diversity Receivers in the Presence of k - μ F ading," in *Proceedings of IEEE conference TELSIKS 2015*, 2015, pp. 271–274.
[12] "Wolfram Functions Site." [Online]. Available: http://functions.wolfram.com. [Accessed: 10-Jun-2016].
[13] J. Li, A. Bose, and Y. Q. Zhao, "Rayleigh flat fading channels' capacity," in *Proceedings of the 3rd Annual Communication Networks and Services Research Conference*, 2005, vol. 2005, pp. 214–217.
[14] P. Varzakas, "Average channel capacity for Rayleigh fading spread spectrum MIMO systems," *Int. J. Commun. Syst.*, vol. 19, no. 10, pp. 1081–1087, 2006.
[15] W. Hu, L. Wang, G. Cai, and G. Chen, "Non-Coherent Capacity of M -ary DCSK Modulation System over Multipath Rayleigh Fading Channels," *IEEE Access*, vol. 5, no. 1, pp. 956–966, 2017.
[16] P. Yang, Y. Wu, and H. Yang, "Capacity of Nakagami- m Fading Channel With BPSK/QPSK Modulations," *IEEE Commun. Lett.*, vol. 21, no. 3, pp. 564–567, 2017.
[17] J. M. Romero-Jerez and F. J. Lopez-Martinez, "Fundamental capacity limits of spectrum-sharing in Hoyt (Nakagami-q) fading channels," in *IEEE Vehicular Technology Conference*, 2017.
[18] D. B. Djosic, D. M. Stefanovic, and C. M. Stefanovic, "Level Crossing Rate of Macro-diversity System with Two Micro-diversity SC Receivers over Correlated Gamma Shadowed α–μ Multipath Fading Channels," *IETE J. Res.*, vol. 62, no. 2, pp. 140–145, 2016.
[19] S. R. Panić, D. M. Stefanović, I. M. Petrović, M. Č. Stefanović, J. A. Anastasov, and D. S. Krstić, "Second-order statistics of selection macro-diversity system operating over Gamma shadowed $κ$-$μ$ fading channels," *EURASIP J. Wirel. Commun. Netw.*, vol. 2011, no. 1, p. 151, Oct. 2011.
[20] P. S. Bithas and A. A. Rontogiannis, "Mobile Communication Systems in the Presence of Fading/Shadowing, Noise and Interference," pp. 1–14, 2014.
[21] M. Stefanović, S. R. Panić, N. Simić, P. Spalević, and Č. Stefanović, "On the macrodiversity reception in the correlated gamma shadowed Nakagami-M fading," *Teh. Vjesn.*, vol. 21, no. 3, pp. 511–515, 2014.
[22] B. Jaksic, M. Stefanovic, D. Aleksic, D. Radenkovic, and S. Minic, "First-Order Statistical Characteristics of Macrodiversity System with Three Microdiversity MRC Receivers in the Presence of κ-μ Short-Term Fading and Gamma Lon," *J. Electr. Comput. Eng.*, vol. 2016, pp. 1–9, 2016.
[23] I. S. Gradshteyn and I. M. Ryzhik, *Table of Integrals, Series, and Products*, 5th ed. Sad Diego: San Diego, Academic Press.
[24] M. S. Alouini and A. J. Goldsmith, "Capacity of Rayleigh fading channels under different adaptive transmission and diversity-combining techniques," *IEEE Trans. Veh. Technol.*, vol. 48, no. 4, pp. 1165–1181, 1999.
[25] N. Y. Ermolova, "Capacity Analysis of Two-Wave with Diffuse Power Fading Channels Using a Mixture of Gamma Distributions," *IEEE Commun. Lett.*, vol. 20, no. 11, pp. 2245–2248, 2016.
[26] B. S. Jakšić, "Level Crossing Rate of Macrodiversity SC Receiver with two Microdiversity SC Receivers over Gamma Shadowed Multipath Fading Channel," *Facta Universitatis, Ser. Autom. Control Robot.*, vol. 14, no. 2, pp. 87–98, Mar. 2015.
[27] A. P. Prudnikov and J. A. Brychkov, *Integrasl and series*, 2nd ed. Moscow: Moscow, Fizmatlit, 2003.